Complex frequency analysis and source of losses in rectangular sonic black holes

Viktor Hruška, Jean-Philippe Groby, Michal Bednařík

Complex frequency analysis and source of losses in rectangular sonic black holes

Viktor Hruška[a], Jean-Philippe Groby[b], Michal Bednařík[a]

[a]*Faculty of Electrical Engineering, Czech Technical University in Prague, Technicka 2, Prague, 166 27, Czech Republic*
[b]*Laboratoire d'Acoustique de l'Université du Mans (LAUM), UMR 6613, Institut d'Acoustique - Graduate School (IA-GS), CNRS, Le Mans Université, France,*

Abstract

The amount and practical source of losses required by rectangular sonic black holes in air to effectively absorb low-frequency sound are analyzed numerically and experimentally. In the sole presence of viscothermal losses, only high-order (high frequency) Fabry-Perrot resonances are likely to be critically coupled in realistic rectangular sonic black holes. This results in sharp absorption peaks that do not reach unity at low frequencies, because the quality factors of the associated resonances are high. To avoid these drawbacks, slits of rectangular sonic black holes are partially filled with porous materials so that a profile of porous filled slits is superimposed on the sonic black hole profile itself. The improvement in the absorption coefficient is significant, particularly at frequencies below the viscous/inertial transition frequency of the porous material. This transition frequency is assumed to be the limit of possible perfect absorption of the bulk porous material layer. The numerical results are supported by experimental results, which also show that the vibrations of the plate forming the acoustic black hole must be considered with caution.

Preprint submitted to Elsevier *November 18, 2024*

Keywords: acoustic black hole, porous material, critical coupling, sonic black hole

1. Introduction

Acoustic black holes are passive devices used for the attenuation of the acoustic energy, which operate by reducing the wave speed. They can be classified according to the type of wave they are used to manipulate, also they share similar underlying principles [1]: either acoustic waves in fluids, usually the air medium, also refereed to as sonic black holes (SBHs), or elastic waves in elastic materials, usually thin elastic plates, also referred to as vibrational black holes (VBHs). In this article, we will focus on SBHs. SBHs are usually implemented as waveguide terminations and consist in a series of resonant elements formed between consecutive thin obstacles (either rectangular plates or axis-symmetric rings) that leads to locally reacting effective impedance boundaries. The wave dispersion induced by the resonances of these elements slows down the wave and, as such, SBHs can be seen as slow sound absorbers (see e.g. [2, 3]). However, slow sound absorbers rely on a small number of subwavelength loading resonators, while SBHs mostly rely on a large number of almost non-resonant (in the usefull frequency range) side branch elements. Effectively, the lowest resonance frequency of resonant elements (i.e., that of the longest quarter-wavelength resonator) created between each obstacles of a SBH usually correspond to the cut-on frequency of the first higher-order mode of the main waveguide. The number of possible Fabry-Perrot (FP) resonances being dictated by the number of side branch resonators at low frequency, the number of FP modes in SBHs is thus very large, notably when compared to

that of slow-sound absorbers. In theory, the wave can be entirely stopped and the SBH is impedance matched to the exterior waveguide thanks to the gradient of resonance. Thus, no energy escapes from the black hole, hence the nomenclature based on astrophysics. Note that this analysis usually relies on a system of infinite depth, i.e., a specific transmission problem. However, the acoustic wave cannot be entirely stopped in practice, because SBH are necessarily of finite depth [4, 5, 6, 7, 8, 9]. A SBH has thus a quantifiable and discrete number of FP modes and as a consequence, the acoustic wave is at best slowed down to a very low value, but the phase speed is never zero. In addition, attenuation mechanism has to be introduced to correctly damped these modes. Slowing down the acoustic wave increases the density of state below the lowest resonant elements, which is in turn associated with an increase of the losses. Unless a particularly advantageous geometry is used (e.g., a long and narrow SBH with a very fine slit structure), additional source of dissipation to inherent viscothermal losses of the SBH is required to achieve broadband absorption, e.g. micro-perforated plates [10], melamine foam [11] and more generally porous materials [5, 12]. The reason of these additional dissipation source is rarely explained. The name "black hole" is thus avoided by some authors, e.g. Červenka and Bednařík [13] prefer the name "sound-absorbing structure" or Umnova et al. [14] prefer the name "metamaterial graded absorber".

The description of the acoustic wave propagation in a SBH is usually based on the generalized Webster equation where the varying effective impedance boundary is accounted for [4]. However, only a few number of analytical solution to this equation are available: either for simple SBH profiles (see e.g.,

[15]) or by approximate methods, such as WKB (see e.g., [7]). Guasch et al. [15, 16] and Sharma et al. [17] employed the transfer matrix method, which may fail in case of large gradient. Hollkamp and Semperlotti [18] mimic the SBH as a fractional order operator. In addition, the dissipation model is a key issue for a correct description of quasi-plane wave propagation in SBH. Originally, Mironov and Pislyakov [4] assumed that the losses inside the SBH could be correctly captured by adding a small constant imaginary part to the sound speed. This approach was further used, e.g., by Mi et al. [9], but the agreement between theoretical and experimental results was rather poor. Guasch et al. [16] proposed an effective metafluid model accounting for the losses and Umnova et al. [14] adopted the framework of porous material acoustics. Červenka and Bednařík [13] argued that a single phenomenological value of an effective complex sound speed representing all the losses cannot capture the underlying physics in a satisfactory manner. For these two main reasons (modelings of spatially varying admittance boundaries and of the dissipation), the propagation of acoustic wave in SBH is often simulated by the finite element method (see e.g., [13, 11]). This approach is also used in the present work.

In the following, we analyze SBH in terms of critical coupling (see e.g., [19, 20, 21]), thus extending the work of Leng et al. [8] to acoustics. Only realistic SBH are considered, i.e., SBH which can be faithfully rapid manufactured. The article is organized as follows. First, we analyze the reflection coefficient of SBHs in the complex frequency plane, i.e., the possibility to meet the critical coupling condition for a real rectangular SBH. Subsequently, increasing the amount of losses by inserting porous material in the

slit is investigated. Finally, a typical SBH, described by the superposition of the profile of the SBH and that of porous filled slits is manufactured by rapid manufacturing technique and tested in a square impedance tube. Measured and numerically calculated absorption coefficients are found in good agreement, also the vibration of the SBH plate is questioned.

2. Description of the configuration and means of analysis

The studied SBH consists of parallel thin plates of different heights arranged perpendicularly in a rigid-walled waveguide of square cross-sectional area filled with air, as shown in Fig. 1(a-b). The lateral dimensions of the waveguide and the frequency range are chosen so that only plane wave can propagate in the waveguide. The open apendicular parts of the plates form an effective admittance boundary that varies continuously along the axis of the waveguide, i.e., along the depth of the SBH. Many more SBH (effective admittance boundary) profiles can be manufactured for sound wave in air than for bending waves in thin elastic plates. We are thus not restricted to the usual polynomial (often quadratic) profiles and can consider profiles with more complicated functions. The main issues concerning the SBH profile are related to its slope and narrowing at the end of the structure to ensure impedance matching to the main waveguide. Hence, we chose a sigmoid function. Specifically, we employ the hyperbolic tangent function:

$$y = 0.97A_0 \frac{\tanh\left(b(x - x_i)\right) + \tanh\left(bx_i\right)}{\tanh\left(b(L - x_i)\right) + \tanh\left(bx_i\right)} \,, \tag{1}$$

where A_0 and L denote the SBH half-height and length, and x_i and b are the location of the inflection point and the parameter governing the slope of the

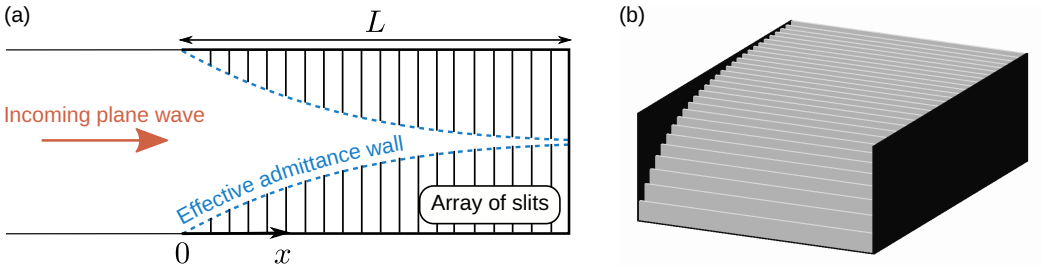

Figure 1: (a) Schematics of the rectangular acoustic black hole for sound waves in air. (b) 3D render of half of a rectangular acoustic black hole.

profile. This expression ensures that $y(0) = 0$, $y(L) = 0.97A_0$, and $y''(x_i) = 0$. The geometry is primarily based on the feasibility of manufacturing the SBH by rapid manufacturing techniques. We deliberately do not choose a convenient aspect ratio of the SBH in order to study a realistic case. The final geometry consists of a $L = 200$ mm depth SBH of 150 mm $\times$ 150 mm cross-sectional area (i.e., $A_0 = 75$ mm). The corresponding cut-off frequency is 1150 Hz.

This boundary profile and the variation of the admittance result in slowing down the quasi-plane wave propagating in the SBH. Thus, the wavelength is shortened and the density of state increases. The increase of the density of state induced by slowing-down the acoustic wave speed is accompanied by an increase of the attenuation. The SBH reflection coefficient is analyzed in the complex frequency plane $\mathcal{F} = f + \mathrm{i}f_i$, where f is the real frequency and f_i is the imaginary part of the complex frequency. The possibility to meet the critical coupling condition for real-life rectangular SBH is examined. When a zero of the reflection coefficient exactly lies on the real frequency axis, the energy leakage is exactly compensated by the loss of the system and perfect absorption is achieved [19, 20, 21]. Note that each zero corresponds to a

mode of the system (both are complex conjugates of each other in the absence of losses). The rectangular SBH exhibit Fabry-Perrot resonances along its depth, but do not, a priori, support trapped modes inside the slits. Effectively, the lowest possible quarter-wavelength resonance frequency of the slit coincides with the cut-on frequency of the first non-planar mode of the main waveguide and is thus out of the considered frequency range. Hence, only the Fabry-Perrot resonances and contributions from evanescent coupling between the slits are expected in rectangular SBHs. This conclusion may be tempered by the shortening of the wavelength along the SBH [13].

3. Complex frequency plane analysis when only viscothermal losses are accounted for

Since the exact model describing the losses in the SBH is still subjected to debat, we simulate the acoustic response of the SBH by solving the whole set of linearized Navier-Stokes equations with no-slip and isothermal boundary conditions on the walls with resolved boundary layers. All boundaries are assumed perfectly rigid (no elastic vibrations were accounted for) and all results are thus simulated with Comsol Multiphysics 5.5 in 2-dimensional configurations because of the symmetry of the considered SBH. The plates are 2.5 mm thick and the slits between each of them are 2.5 mm thick as well.

We numerically studied the influence of the SBH profile on the possibility of critically coupling the SBH to a normal incident wave when only viscothermal losses are accounted for. The time Fourier convention is $e^{\mathrm{i}\omega t}$, where $\omega = 2\pi f$ is the pulsation.

Fig. 2 (a) depicts the locations of the poles and zeros of the reflection coefficient in the complex frequency plane for different positions of the profile inflection point x_i. The slope is fixed at $b = 20$ m^{-1}. The corresponding profiles are depicted Fig. 2 (b). Generally, the smaller x_i is, i.e., the longer the narrow portion is, the lower the resonance frequencies are. In details, the smaller x_i is, the closer the poles and zeros are to the real frequency axis. In other words, the smaller x_i is, the larger the quality factor of the Fabry-Perot mode is and thus the sharper are the associated absorption peaks, see Fig. 2 (c) for example with $x_i = 0$. The SBH acts as a comb filter at least in the lower frequency range. Although the trend is not clear, the higher the frequency, the higher the quality factor, but close to the cut-on frequency of the next order mode of the waveguide. The higher the frequency, the wider the absorption peak, e.g. Fig. 2 (c), thus offering the possibility of the absorption peaks to overlap. In the opposite, the modal density, i.e., the density of state, significantly increases below the cut-on frequency of the first order mode of the waveguide, that is below the lowest frequency quarter-wavelength resonance of the slits. The group velocity vanishes at this frequency and thus the number of Fabry-Perot mode increases to form an accumulation point [22]. The accumulation moderate the high quality factor of the modes located in this frequency range and the absorption present a kind of plateau because the peaks overlap. The fifth modes seem to be or to be nearly critically coupled whatever the position of the inflection point, i.e. the fifth zero of the refection coefficient is located on or close to the real frequency axis (see Fig. 2 (a) around 800 – 1000 Hz), leading to a prefect absorption peak. The lowest frequency modes do not appear to be critically

coupleable because of a lack of losses, i.e. the first four zeros are located in the lower half complex frequency plane. In the opposite, the higher frequency modes do not appear to be critically coupleable because of an excess of losses, i.e., the zeros higher than the fifth zero are usually located in the upper half complex frequency plane. None of the other absorption peaks are perfect.

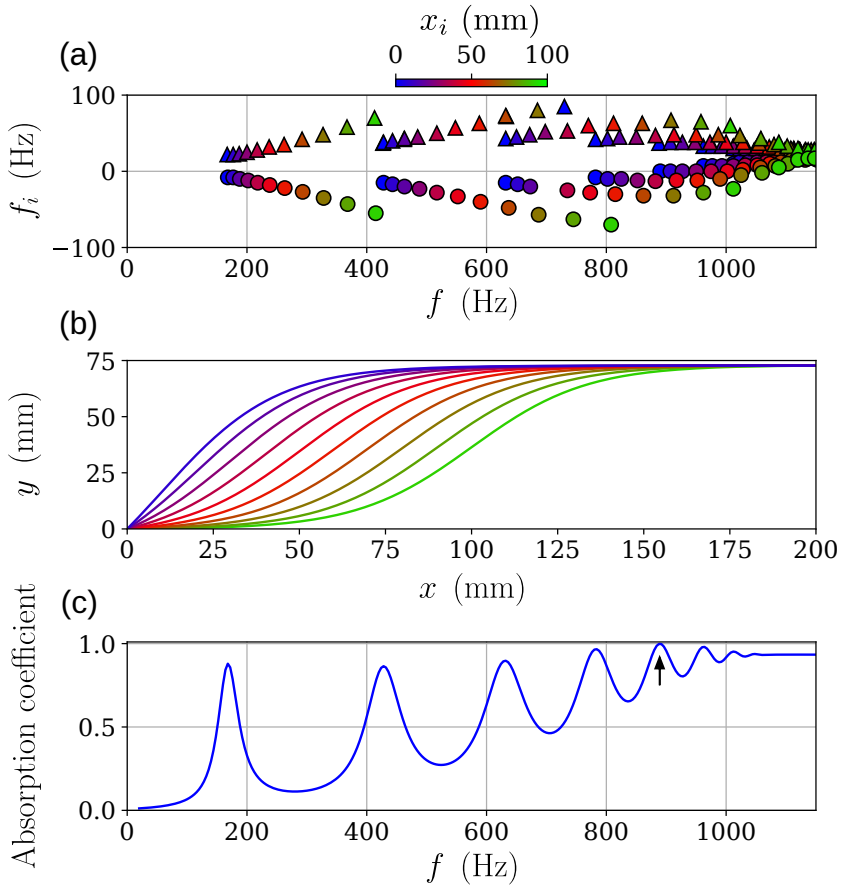

Figure 2: (a) Evolution of poles (△) and zeros (○) when the SBH inflection point varies. (b) Corresponding SBH profiles (heights of the slits). (c) Absorption coefficient for $x_i = 0$ and $b = 20\text{m}^{-1}$. Critical coupling at 890 Hz is marked with an arrow.

Figure 3 (a) depicts the locations of the poles and zeros of the reflection

coefficient in the complex frequency plane for different profile slopes. The position of the inflection point is fixed at $x_i = 60$ mm. The corresponding profiles are depicted Fig. 3 (b). The higher the slope is, i.e., the longer the narrow portion is, the lower the resonance frequencies are. Similar conclusions to those drawn for the effect of decreasing inflection point can be drawn for the effect of increasing slope.

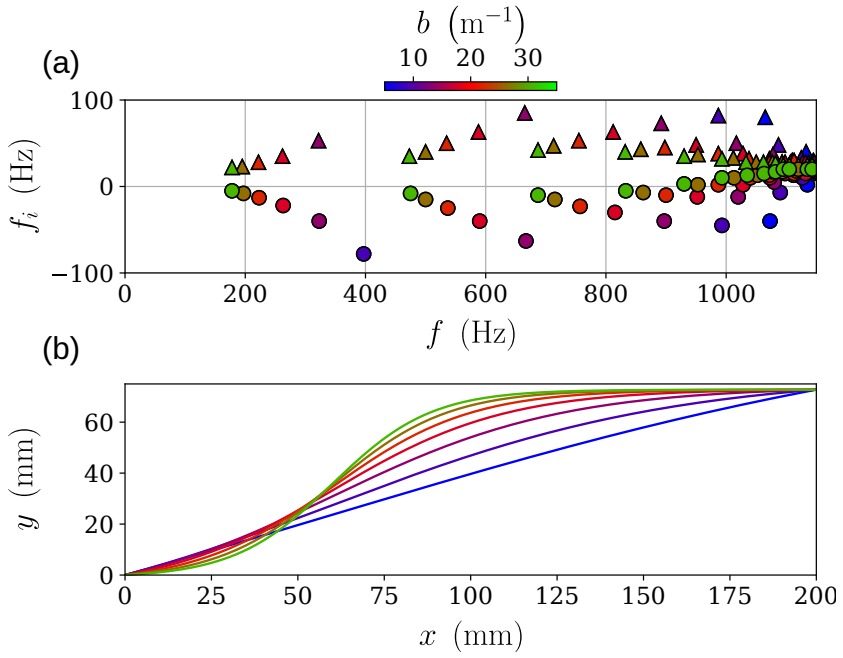

Figure 3: (a) Evolution of poles (△) and zeros (○) when the SBH slope varies. (b) Corresponding SBH profiles (heights of the slits).

The above mentioned results shows that decreasing the inflection point position or increasing the slop have similar impact on the zero and pole locations in the complex frequency plane. These two actions increase the narrow portion length, which is loaded by the longest slits. Nevertheless, the previous results also clearly show that the lowest frequency modes can

hardly be critically coupled because the viscothermal losses are too small in practical SBHs. Reducing the width of the slits and of the plates will increase the amount of losses at low frequency, but the practical realization becomes very difficult. Thus, we propose to fill part of the slits by a porous material, this filling following another profile.

4. Adding a porous materials in the slits to increase the losses

In this section, the numerical simulations are based on the Helmholtz equation for acoustic pressure with the use of the effective parameters (density and compressibility) given by Johnson-Champoux-Allard-Lafarge [23, 24] to model the propagation in the porous material and those given by Stinson [25] to model that in the slits filled with air in the presence of viscothermal losses. These approximations in the losses and propagation models are assumed not impacting the results, because most of the energy dissipation is assumed to occur in the porous materials. The SBH now relies on two profiles. The first profile governs the SBH itself and the second profile governs the slits that are filled with porous materials. For simplicity, the latter profile also follows a hyperbolic tangent curve given by Eq.(1) where the parameters are identified by the exponent p. The resulting SBH is depicted in Fig. 4(a). These two profiles are highest against a rigid end of the SBH where the highest slits are located. Indeed, energy attenuation occurs at the end of the SBH at low frequencies, and closer to the aperture as the frequency increases. The goal being to study the impact of filling part of the slits with porous materials, we did not optimize the design but rather present a representative design. The parameters of the porous material are given in Table 1 and were

ϕ	α_∞	Λ (μm)	Λ' (μm)	k_0 ($\times 10^{-9}$m^2)	k_0' ($\times 10^{-9}$m^2)
0.99	1	142	244	3.1877	4.5866

Table 1: Porous material parameters (see e.g., [26] for the meaning of the individual symbols).

experimentally measured in a 3 cm-diameter impedance tube following the procedure described in [26]. The porous material is a foam that is usually considered as an isotropic medium. The plate thickness is fixed at 2 mm, while the slit thickness is now fixed at 5 mm. The slits are thicker to ensure the porous material can be modeled as a homogeneous porous material (i.e., several pores should be present in the slit thickness) and to ease the porous lamella insertion. The resulting SBH geometric parameters are $A_0 = 75$ mm, $L = 200$ mm, $b = 20$ m^{-1}, and $x_i = 0$ for the SBH profile, and $A_0^p = 75$ mm, $L^p = 200$ mm, $b^p = 25$ m^{-1}, and $x_i^p = 100$ mm for the porous material profile filling the slits. The structure was then manufactured by stereolithography from epoxy resine and porous material lamellas, previously sliced with a band saw, were inserted in the slits according to the porous material profile. Figure 4(b) presents the manufactured sample. The reflection coefficient of the SBH was measured in an impedance tube of square cross-sectional area (see Fig. 4(c)) using a microphone fixed on a robotized arm inside the tube, following the procedure described in [27, 3]. The excitation is a sweap sine function from 100 Hz to 1250 Hz with a sampling frequency of 5 Hz. The data were acquired with a Zurich Instruments MFIA. Each measurements are averaged over 100 cycles.

Figure 5(a) depicts the absorption coefficient as simulated and as mea-

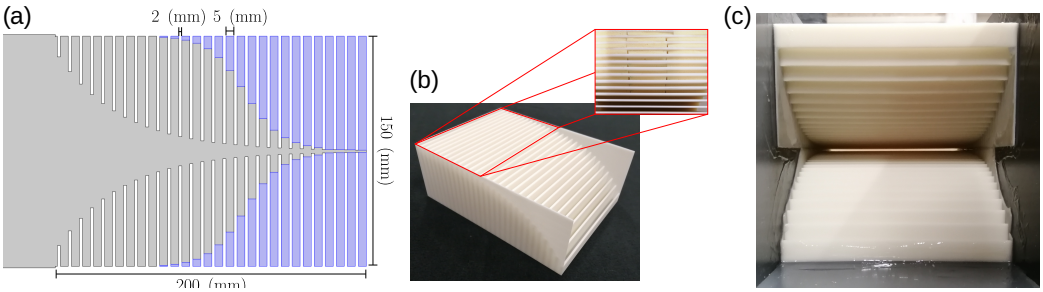

Figure 4: Geometry of the studied SBH with partial porous filling (marked in blue).

sured and Figure 5(b) depicts the absolute value of the corresponding reflection coefficient in the complex frequency plane. The locations of the zeros are in good agreement with the absorption peaks. Of particular interest is the fact that the lowest frequency mode is almost critically coupled, leading to an almost perfect absorption peak around 160 Hz. Once again, this configuration was not optimized but improvement with respect to the configuration in the absence of the porous material is clear, see Fig. 5(c). The quality factors of the higher frequency modes are lower resulting in a smoother and flatter absorption coefficient for frequencies higher than 400 Hz. This SBH absorption efficiency is higher than that of a bulk layer of the same homogeneous porous material that partially fills the slits and of the the same thickness. Effectively, perfect absorption can only be reached in case of bulk porous material layer when the quarter-wavelength resonance frequency is slightly higher than the viscous-inertial transition frequency [28], i.e., the Biot's frequency. This means that perfect absorption is theoretically impossible below $\approx$ 750 Hz and would require a $\approx$ 11 cm-thick layer. In our case, we achieve almost perfect absorption around 160 Hz. Please note that the zeros garland in Fig. 5(b) is composed of two branches with an inflection point around

850 Hz. At this frequency another type of mode, with a lower quality factor appears (the wide blue spot). This frequency is also very close to the viscous-inertial transition frequency.

Although the agreement between the experiment and the simulation results is very good, an additional absorption peak was measured around 210 Hz. Three-dimensional acoustic simulations (depicted with red dots in Fig. 5(a)) and vibroacoustic eigenfrequency analysis were conducted. Figure 5(c) depicts the modal shapes of the first three vibrational modes of the highest plate (i.e., that located at the end of SBH). The plate is clamped at both lateral sides and at the bottom side, while free at the top side. The frequency of the first mode correspond in good approximation to that of the additional absorption peak. Around the frequency of the third mode, ripples were measured, as can be noticed in Fig. 5(a). The second plate mode cannot be excited because of symmetry reason. The experimental discrepancies are also attributed to the vibration of the deepest and highest plates. Although not expected, the plate vibration appears as a drawback, in the sense that it requires vibroacoustic modeling, but also as a benefit, in the sense that it leads to additional absorption peak. This vibroacoustic coupling was to be expected, as the plates are poorly supported in case of rectangular SBH, especially in case of large width. Either thicker or higher mass plates, or supports between the plates have to be added to diminish this vibroacoustic effect.

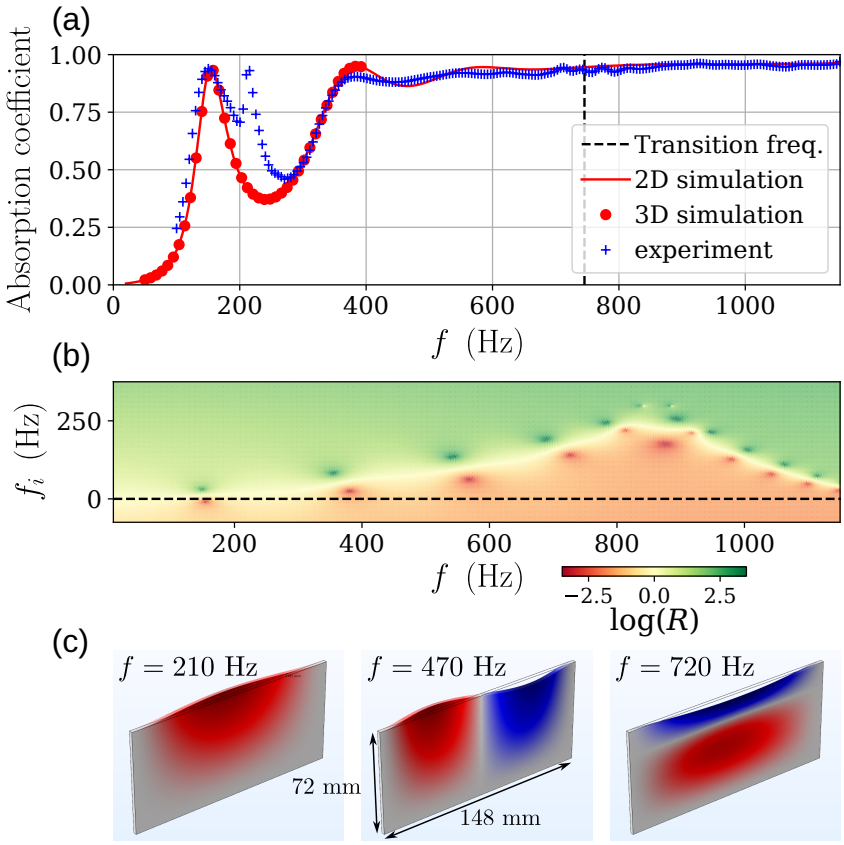

Figure 5: (a) Absorption coefficient of the SBH with partial porous filling. Comparison of experimental data (blue crosses) and numerical simulations in 2D (red line) and 3D (red dots). (b) Corresponding reflection coefficient in the complex frequency plane. (c) Three lowest vibrational modes of a single (rear) SBH plate.

5. Conclusions

The absorption efficiency of realistic rectangular sonic black holes (SBH) is analyzed thanks to the representation of the reflection coefficient (eigenvalue of the scattering matrix) in the complex frequency plane. The degree of freedom offered to SBH in relation to vibroacoustic black holes is used in analyze the impact of different profiles on the possibly to critically couple

these SBH to the impinging wave. Critically coupling the lowest frequency Fabry-Perot resonance with the unique viscothermal losses is found almost impossible for realistic SBH, i.e., thickness of the slit of the order of a few millimeters. The reason is clearly a lack of losses. To fix this issue, we superimposed a second profile of partially filled with a usual (close to melamine) porous material slits. The SBH is then characterize by two profiles: the first one that described the SBH itself, and the second one that governs the partially filled with porous material slits. The highest location of both profiles is close to the rigid backing, i.e., the end of the SBH, because dissipation occurs mostly at the end of the SBH at low frequency. The absorption coefficient of the partially filled with porous material SBH is significantly improved when compared to the same SBH in the absence of porous materials. A typical (in the sense that we do not optimize the structure) SBH is manufactured, slits are partially filled with porous materials, and tested in a square impedance tube. The measured and simulated results are found in good agreement. Although the rigid obstacles were chosen reasonably thick, an additional absorption peak is measured because of the vibration of the highest obstacles. This pave the way of perfectly absorbing SBH combining vibroacoustic and sonic aspects, that will be optimized and manufactured.

Acknowledgement

This work was supported by the Grant Agency of the Czech Republic (GACR) grant No. 22-33896S and the ANR 17-EURE-0014 project. JPG would like to acknowledge the financial support of ANR-RGC METARoom (Grant No. ANR-18-CE08-0021).

References

[1] A. Pelat, F. Gautier, S. C. Conlon, F. Semperlotti, The acoustic black hole: A review of theory and applications, Journal of Sound and Vibration 476 (2020) 115316. doi:10.1016/j.jsv.2020.115316.

[2] J.-P. Groby, W. Huang, A. Lardeau, Y. Aurégan, The use of slow waves to design simple sound absorbing materials, Journal of Applied Physics 117 (12) (03 2015). doi:10.1063/1.4915115.

[3] N. Jiménez, V. Romero-García, V. Pagneux, J.-P. Groby, Rainbow-trapping absorbers: Broadband, perfect and asymmetric sound absorption by subwavelength panels for transmission problems, Scientific Reports 7 (1) (Oct. 2017). doi:10.1038/s41598-017-13706-4.

[4] M. A. Mironov, V. V. Pislyakov, One-dimensional acoustic waves in retarding structures with propagation velocity tending to zero, Acoustical Physics 48 (3) (2002) 347–352. doi:10.1134/1.1478121.

[5] A. Azbaid El Ouahabi, V. Krylov, D. O'Boy, Experimental investigation of the acoustic black hole for sound absorption in air, in: 22nd International Congress on Sound and Vibration, Florence, Italy, 2015.

[6] A. Azbaid El Ouahabi, V. Krylov, D. O'Boy, Investigation of the acoustic black hole termination for sound waves propagating in cylindrical waveguides, in: International Conference 'InterNoise 2015', San Francisco, USA, 2015.

[7] M. Mironov, V. Pislyakov, One-dimensional sonic black holes: Exact

analytical solution and experiments, Journal of Sound and Vibration 473 (2020) 115223. doi:10.1016/j.jsv.2020.115223.

[8] J. Leng, V. Romero-García, A. Pelat, R. Picó, J.-P. Groby, F. Gautier, Interpretation of the acoustic black hole effect based on the concept of critical coupling, Journal of Sound and Vibration 471 (2020) 115199. doi:10.1016/j.jsv.2020.115199.

[9] Y. Mi, W. Zhai, L. Cheng, C. Xi, X. Yu, Wave trapping by acoustic black hole: Simultaneous reduction of sound reflection and transmission, Applied Physics Letters 118 (11) (2021) 114101. doi:10.1063/5.0042514.

[10] X. Zhang, L. Cheng, Broadband and low frequency sound absorption by sonic black holes with micro-perforated boundaries, Journal of Sound and Vibration 512 (2021) 116401. doi:10.1016/j.jsv.2021.116401.

[11] A. Mousavi, M. Berggren, E. Wadbro, How the waveguide acoustic black hole works: A study of possible damping mechanisms, The Journal of the Acoustical Society of America 151 (6) (2022) 4279–4290. doi:10.1121/10.0011788.

[12] A. S. Elliott, R. Venegas, J. P. Groby, O. Umnova, Omnidirectional acoustic absorber with a porous core and a metamaterial matching layer, Journal of Applied Physics 115 (20) (2014) 204902. doi:10.1063/1.4876119.

[13] M. Červenka, M. Bednařík, On the role of resonance and thermoviscous losses in an implementation of “acoustic black hole”

for sound absorption in air, Wave Motion 114 (2022) 103039. doi:10.1016/j.wavemoti.2022.103039.

[14] O. Umnova, D. Brooke, P. Leclaire, T. Dupont, Multiple resonances in lossy acoustic black holes - theory and experiment, Journal of Sound and Vibration 543 (2023) 117377. doi:10.1016/j.jsv.2022.117377.

[15] O. Guasch, M. Arnela, P. Sánchez-Martín, Transfer matrices to characterize linear and quadratic acoustic black holes in duct terminations, Journal of Sound and Vibration 395 (2017) 65–79. doi:10.1016/j.jsv.2017.02.007.

[16] O. Guasch, P. Sánchez-Martín, D. Ghilardi, Application of the transfer matrix approximation for wave propagation in a metafluid representing an acoustic black hole duct termination, Applied Mathematical Modelling 77 (2020) 1881–1893. doi:10.1016/j.apm.2019.09.039.

[17] N. Sharma, O. Umnova, A. Moorhouse, Low frequency sound absorption through a muffler with metamaterial lining, in: 24th International congress of sound and vibration, London, 2017.

[18] J. P. Hollkamp, F. Semperlotti, Application of fractional order operators to the simulation of ducts with acoustic black hole terminations, Journal of Sound and Vibration 465 (2020) 115035. doi:10.1016/j.jsv.2019.115035.

[19] J.-P. Groby, R. Pommier, Y. Aurégan, Use of slow sound to design perfect and broadband passive sound absorbing materials, The Jour-

nal of the Acoustical Society of America 139 (4) (2016) 1660–1671. doi:10.1121/1.4945101.

[20] V. Romero-García, G. Theocharis, O. Richoux, V. Pagneux, Use of complex frequency plane to design broadband and sub-wavelength absorbers, The Journal of the Acoustical Society of America 139 (6) (2016) 3395–3403. doi:10.1121/1.4950708.

[21] V. Romero-García, G. Theocharis, O. Richoux, A. Merkel, V. Tournat, V. Pagneux, Perfect and broadband acoustic absorption by critically coupled sub-wavelength resonators, Scientific Reports 6 (1) (Jan. 2016). doi:10.1038/srep19519.

[22] N. Jiménez, V. Romero-García, V. Pagneux, J.-P. Groby, Quasiperfect absorption by subwavelength acoustic panels in transmission using accumulation of resonances due to slow sound, Phys. Rev. B 95 (2017) 014205. doi:10.1103/PhysRevB.95.014205.

[23] D. L. Johnson, J. Koplik, R. Dashen, Theory of dynamic permeability and tortuosity in fluid-saturated porous media, Journal of Fluid Mechanics 176 (1987) 379–402. doi:10.1017/S0022112087000727.

[24] D. Lafarge, P. Lemarinier, J. F. Allard, V. Tarnow, Dynamic compressibility of air in porous structures at audible frequencies, The Journal of the Acoustical Society of America 102 (4) (1997) 1995–2006. doi:10.1121/1.419690.

[25] M. R. Stinson, The propagation of plane sound waves in narrow and wide circular tubes, and generalization to uniform tubes of arbitrary

cross-sectional shape, The Journal of the Acoustical Society of America 89 (1991) 550–558.

[26] M. Niskanen, J.-P. Groby, A. Duclos, O. Dazel, J. C. L. Roux, N. Poulain, T. Huttunen, T. Lähivaara, Deterministic and statistical characterization of rigid frame porous materials from impedance tube measurements, The Journal of the Acoustical Society of America 142 (4) (2017) 2407–2418. doi:10.1121/1.5008742.

[27] J.-P. Groby, W. Lauriks, T. E. Vigran, Total absorption peak by use of a rigid frame porous layer backed by a rigid multi-irregularities grating, The Journal of the Acoustical Society of America 127 (5) (2010) 2865–2874. doi:10.1121/1.3337235.

[28] N. Jiménez, V. Romero-García, J.-P. Groby, Perfect absorption of sound by rigidly-backed high-porous materials, Acta Acustica united with Acustica 104 (2018) 396–409. doi:10.3813/AAA.919183.